The American Journal of Pathology, Vol. 175, No. 4, October 2009

DOI: 10.2353/ajpath.2009.090091

Tumorigenesis and Neoplastic Progression

Epigenetic Silencing of *Stk39* in B-Cell Lymphoma Inhibits Apoptosis from Genotoxic Stress

Cynthia E. Balatoni,* David W. Dawson,*† Jane Suh,* Mara H. Sherman,‡ Grant Sanders,* Jason S. Hong,* Matthew J. Frank,* Cindy S. Malone,¶ Jonathan W. Said,* and Michael A. Teitell*†‡§‖

From the Department of Pathology and Laboratory Medicine, Jonsson Comprehensive Cancer Center,† and Eli and Edythe Broad Center of Regenerative Medicine and Stem Cell Research,§ David Geffen School of Medicine at UCLA, Los Angeles, California; Department of Biology, California State University Northridge, Northridge, California¶; and Molecular Biology Institute‡ and California NanoSystems Institute,‖ UCLA, Los Angeles, California*

B-cell lymphomas, the most frequent human immune system malignancies, often contain dysregulated *TCL1* oncogene expression. *TCL1* transgenic (TCL1-tg) mice develop a spectrum of B-cell malignancies, supporting an oncogenic role for TCL1 in B cells. Our prior global survey of DNA methylation patterns in TCL1-tg B-cell lymphomas identified many lymphoma-specific candidate hypermethylated genes, including *Stk39*. The *Stk39* encoded protein, sterile 20-like-related proline-alanine-rich kinase (SPAK), regulates cell stress responses, and microarray studies identified reduced SPAK expression in metastatic prostate and treatment-resistant breast cancers, suggesting that its loss may have a role in cancer progression. Here we identified DNA hypermethylation and SPAK silencing in TCL1-tg B-cell lymphomas and SPAK silencing without DNA methylation in multiple subtypes of human B-cell lymphomas. SPAK knockdown by shRNA protected B cells from caspase-dependent apoptosis induced by DNA double-strand breaks but not apoptosis in response to osmotic or oxidative cell stressors. Caspase 3 activation by cleavage was impaired with SPAK repression in DNA damaged B cells. Interestingly, c-Jun NH_2-terminal kinase is potentially activated by SPAK and pharmacological inhibition of c-Jun NH_2-terminal kinase in SPAK-expressing B cells recapitulated the cell-protective phenotype of SPAK knockdown. Taken together, these data indicate that SPAK loss in B-cell lymphomas promotes increased cell survival with DNA damage and provides a potential mechanism for increased resistance to genotoxic stress in cancer. ***(Am J Pathol 2009, 175:1653–1661; DOI: 10.2353/ajpath.2009.090091)***

Leukemias and lymphomas arise by genetic and epigenetic alterations of previously healthy lymphocytes. B-cell lymphoma is the most frequent lymphocyte malignancy, with certain tumor subtypes characterized by recurring genetic alterations that include reciprocal chromosome translocations between *IG* loci and *CCND1*, *BCL2*, *MYC*, and *BCL6*.[1] These rearrangements place tumor-promoting genes under the control of *IG* rather than endogenous regulatory elements, leading to their dysregulated expression. Epigenetic changes, including DNA hypermethylation, aberrant histone modifications, and altered microRNA expression are also linked to B-cell transformation.[2–4] In particular, DNA hypermethylation promotes chromatin compaction and gene silencing, with consistent repression of specific tumor suppressor genes associated with multiple types of cancer, including subtypes of B-cell leukemia and lymphoma.[5]

Aberrant expression of the *TCL1* oncogene, first identified from rearrangements with *TCR* loci in T-cell prolymphocytic leukemia, also occurs frequently in mature B-cell leukemias and lymphomas, although not by gene rearrangement [reviewed in[6]]. A causative role for ectopic *TCL1* expression in lymphocyte transformation is supported by three different *TCL1* transgenic (TCL1-tg) mouse models that develop mature B- and T-cell malignancies.[6,7] TCL1-tg mice and patients with dysregulated *TCL1* expression exhibit polyclonal lymphocyte hyperplasia and a long delay to tumor formation,

Supported by National Institutes of Health grants T32CA009120, R01CA90571, R01CA107300, R01GM073981, R15GM080683, and PN2EY018228. M.A.T. is a Scholar of the Leukemia and Lymphoma Society.

Accepted for publication June 18, 2009.

Supplemental material for this article can be found on *http://ajp.amjpathol.org*.

Address reprint requests to Dr. Michael Teitell, M.D., Ph.D., Department of Pathology, 10833 Le Conte Avenue, Los Angeles, CA 90095. E-mail: mteitell@ucla.edu.

suggesting that additional genetic or epigenetic lesions are required for transformation.[7] Supporting this idea, our prior work identified companion chromosomal translocations, aneuploidy, and *Myc* overexpression in TCL1-tg B-cell lymphomas.[8] To elucidate epigenetic alterations that accompany and may facilitate transformation or lymphoma progression, unbiased genome-wide DNA methylation analysis of more than 2000 genetic loci using restriction landmark genomic scanning (RLGS) was performed and demonstrated reproducible nonrandom patterns of aberrant DNA methylation in TCL1-tg B-cell lymphomas compared with wild-type or nontransformed TCL1-tg B cells.[9] This RLGS survey detected tumor-associated hypermethylation of 115 candidate loci including two loci belonging to serine/threonine protein kinase 39 (*Stk39*).

STK39 encodes STE20 (sterile 20-like)-related proline-alanine-rich kinase (SPAK), one of two members of the germinal center kinase VI subgroup within the STE20 kinase family.[10] In general, mammalian STE20 kinases are implicated in osmotic stress signaling. SPAK is a 60-kDa protein that contains an N-terminal PAPA box of unknown function, a serine/threonine kinase domain, a putative nuclear localization signal, and a C-terminal region that binds to SPAK target proteins. SPAK is ubiquitously expressed and modulates ion and fluid homeostasis through interactions with and direct phosphorylation of the cation chloride cotransporters KCC3, NKCC1, and NKCC2.[11] Interestingly, SPAK activates the p38 mitogen-activated protein kinase (MAPK) signaling pathway independent of its target binding C-terminal region. c-Jun NH_2-terminal kinase (JNK) MAPK may also be a direct SPAK target, implying an independent SPAK function as an upstream MAP4K.[12]

Expression microarray studies have identified a correlation between reduced *STK39* expression in prostate cancer metastasis and in tumor relapse and resistance to certain treatments in breast cancer.[13,14] However, these studies did not independently validate these microarray results nor did they correlate the loss of *STK39* with tumor progression. Likewise, the role of SPAK in B cells or in B-cell tumors is not known, prompting us to further investigate *Stk39* and SPAK. Here we show that SPAK expression is repressed or silenced in TCL1-tg B-cell tumors and that reduced expression is accompanied by *Stk39* DNA hypermethylation. Moreover, loss of SPAK expression was observed among several primary human B-cell lymphoma subtypes, suggesting that SPAK loss may be a shared feature of both human disease and the *Eμ-B29-hTCL1* mouse model of lymphoma. We show that decreased SPAK expression protected B cells from apoptosis induced by DNA double-strand breaks (DSBs) through a mechanism dependent on caspase activation. This protection was independent of known SPAK downstream effectors, including p38 and the cation chloride cotransporter proteins. Loss of SPAK expression increases the survival of B cells with DNA DSBs, which can occur with specific genotoxic stressors or during a T-cell-dependent germinal center (GC) reaction. By increasing survival, impaired signaling from SPAK loss may promote malignant progression by abrogating the elimination of DNA-damaged B cells and possibly other cell types with DNA damage as well.

Materials and Methods

Mouse Tumor Samples and Cell Lines

TCL1-tg B-cell tumors were from spleens of 9- to 16-month-old mice.[7] Tumor sample Burkitt-like lymphoma (BLL) 1a is a daughter tumor that arose at 6 weeks from adoptive transfer of a primary TCL1-tg B-cell tumor (BLL1) into a 4-month-old syngeneic mouse. All other TCL1-tg B-cell tumors were from the primary source mice. Nalm6 and BCBL1 B cells were grown in RPMI 1640 and HEK293T cells were grown in Dulbecco's modified Eagle's medium plus 10% fetal bovine serum.

Human Lymphomas and Immunohistochemistry

Lymphomas were examined by histology and immunophenotype, classified according to the World Health Organization system, and retrieved from the files of the UCLA Department of Pathology.[15] SPAK antiserum (L. Harrison, Parkville, VIC, Australia) was used at 1:1000 dilution and tumor cell staining was scored on a 0 to 4+ scale in increments of 25% by two pathologists.[16] SPAK expression was detected using the Lab Vision Ultravision ONE Polymer Immunohistochemistry Detection System (Fisher Scientific, Pittsburgh, PA) with horseradish peroxidase (HRP) and DAB Chromogen and a hematoxylin counterstain. In brief, after deparaffinization, rehydration, and antigen retrieval using a vegetable steamer, slides were blocked and incubated overnight at 4°C with rabbit antisera specific for SPAK.

Genomic DNA and Genomic Bisulfite Sequencing

Genomic DNA was isolated from fresh-frozen TCL1-tg B-cell lymphomas or control spleens using TRIzol (Invitrogen, Carlsbad, CA). PCR reactions of 40 cycles were performed on sodium bisulfite-treated genomic DNA, which was prepared as described previously.[17] Agarose gel-purified amplicons were cloned into the pCR2.1-TOPO vector (Invitrogen) with clones isolated and sequenced. PCR primers for bisulfite-converted gDNA were *Stk39* forward (5′-AAGTGTTTTTGAATAAAAGAGAAAGT-3′) and *Stk39* reverse (5′-AAAAAACCCCCCTAAAA-CTCC-3′). The PCR-amplified product spanned the region −229 to +73 upstream of the major *Stk39* transcriptional start site and was 302 nucleotides long (http://genome.ucsc.edu).

Quantitative PCR

RNA was extracted using TRIzol and first-strand cDNA was synthesized using the SuperScript First-Strand Synthesis System (Invitrogen). SYBR green quantitative PCR was performed using an Applied Biosystems 7700 sequence detector. Samples were analyzed for *Stk39* and

the housekeeping gene *36b4* (*Rplp0*). The primers for human and mouse *STK39* and *36B4* were as follows: *hSTK39* forward (5′-GCCATCCCAACGTAGTGACC-3′), *hSTK39* reverse (5′-TGTTCT-CCTCGGTTGACAATGTA-3′), *h36B4* forward (5′-CCCGCTGCTGAACATGCT-3′), *h36B4* reverse (5′-TCGAACACCTGCTGGATGAC-3′), *mSTK39* forward (5′-GCGTAGCCATAAAG-CGGATC-3′), *mSTK39* reverse (5′-TACGTTGGGATGGCTGCATT-3′), *m36B4* forward (5′-AGATGCAGCAGATCCGCAT-3′), and *m36B4* reverse (5′-GTTCTTGCCCATCAGCACC-3′). Each sample was examined in triplicate with a two-tailed *t*-test to determine statistical significance.

Lymphocyte Isolation

Mouse B cells were isolated using an AUTOMACS Cell Sorter (Miltenyi Biotech, Auburn, CA). Incubation with CD4-phycoerythrin (PE), CD8-PE, and Gr1-PE antibodies (BD Pharmingen, San Diego, CA) was followed with anti-PE microbeads (Miltenyi Biotech). B cells were collected by negative selection, with all other cells eluted as the non-B-cell fraction. Tonsillar B cells were isolated and sorted into naive, memory, and germinal center subpopulations, as described previously.[16]

shRNA Vectors, Retroviruses, and Stably Transduced Cell Lines

Three *STK39* shRNA vectors, RNAi1 (5′-GGTGGATGGTCAC-GATGTA-3′), RNAi2 (5′-ATTCAAGCCATGAGTCAGT-3′), and RNAi3 (5′-GAGCAGCGCCTTATCACAA-3′),[18] were generated by cloning DNA oligomers (Dharmacon, Lafayette, CO) into the H1 promoter-driven retroviral plasmid pQSuper (S. Smale, UCLA). To generate retroviruses, HEK293T fibroblasts were transfected overnight using Lipofectamine 2000 (Invitrogen) with 12 μg of each shRNA construct, 4 μg of murine leukemia virus gag/pol pHIT60, and 2 μg of vesicular stomatitis virus glycoprotein. Retrovirus-containing media was collected every 12 hours for 72 hours, and 8 μg/ml Polybrene was added. B-cell lines (1×10^5/ml) were spin-infected at 2500 rpm for 1 hour at 30°C and resuspended in fresh media. Two days later, cells were placed on 1 μg/ml puromycin selection.

Western Blot and Densitometry

Cells were washed twice in 1× PBS, pH 7.4, and lysed in Triton X-100 1× cell lysis buffer (9803; Cell Signaling Technology, Danvers, MA) supplemented with 1 mmol/L phenylmethylsulfonyl fluoride. The 1× lysis buffer contained 20 mmol/L Tris-HCl (pH 7.5), 150 mmol/L NaCl, 1 mmol/L Na_2EDTA, 1 mmol/L EGTA, 1% Triton, 2.5 mmol/L sodium pyrophosphate, 1 mmol/L β-glycerophosphate, 1 mmol/L Na_3VO_4, and 1 μg/ml leupeptin. Protein lysates (40 μg) were resolved by 3% stacking/8% resolving SDS-polyacrylamide gel electrophoresis, transferred to nitrocellulose membranes, incubated for 1 hour with 5% milk Tris-buffered saline-Tween 20 and overnight with primary antibodies in 5% BSA. Antibodies from Cell Signaling Technology were the following: SPAK (1:1000) (2281), OSR1 (1:1000) (3729), caspase 3 (1:1000) (9662), phospho-SAPK/JNK (Thr183/Tyr185) (1:500) (9255), phospho-p53 (Ser15) (1:1000) (9284), and anti-mouse-IgG-HRP (1:5000) (7076). Antibodies from Sigma-Aldrich (St. Louis, MO) were β-tubulin (1:1000) (T-4026) and actin (1:20,000) (A-2066). Anti-rabbit-HRP (1:5000) (711-035-152) was from Jackson ImmunoResearch Laboratories, Inc. (West Grove, PA). ECL reagent (RPN 2209; GE Healthcare, Piscataway, NJ) was used for chemiluminescent detection. Densitometry was performed using SynGene Analysis software (SynGene, Upland, CA).

Drug Treatments and Flow Cytometry

Nalm6 or BCBL1 B cells were seeded at 5×10^5 cells/ml and preincubated for 1 hour with Q-VD-OPH (MP Biomedicals, Solon, OH), furosemide or bumetanide (Sigma-Aldrich), SP600125 (JNK inhibitor), SB203580 (p38 inhibitor), or U0126 (mitogen-activated protein kinase kinase-1/2 inhibitor) (Calbiochem, San Diego, CA). Drug concentrations and incubation times are provided in the figure legends for each experiment. Cells were exposed to ionizing radiation (IR) using a Cs-137 Mark I Irradiator, exposed to UV-B using a Spectrolinker XL-1000 crosslinker (Spectronics Corporation, Westbury, NY), or incubated with etoposide, hydrogen peroxide, or sorbitol (Sigma-Aldrich). Apoptosis was measured using annexin V-FITC and propidium iodide permeability (BD Pharmingen). Vital staining was quantified using a Becton DickInson FACScan analytic flow cytometer, and data were analyzed using CellQuest software (BD Biosciences, San Jose, CA). Each flow cytometry sample was examined in triplicate with a two-tailed *t*-test to determine statistical significance.

Results

DNA Hypermethylation and Repression of Stk39 *Expression in TCL1-tg B-Cell Lymphomas*

Previously, RLGS profiling of genome-wide DNA methylation patterns in TCL1-tg B-cell tumors identified *Stk39* as a candidate hypermethylated gene.[9] *Stk39* was chosen from the list of candidate hypermethylated genes for further study because of its potential loss in cancer progression and its known role in hyperosmotic cell stress responses.[11] Supporting this reasoning, hyperosmotic stress induces cell cycle arrest, mitotic catastrophe, and apoptosis of colonic and pancreatic cancer cells,[19] suggesting a potential role for *Stk39* silencing in lymphoma progression. Genomic bisulfite sequencing of a 255-bp stretch containing 19 CpG sites in a *Stk39* promoter CpG island was performed to assess the extent of DNA methylation and validate the RLGS data (Figure 1A). This region was selected for study because it was part of a larger CpG island that extended into the transcribed region of the gene and because bisulfite sequencing primers could be optimally designed at this site. Only 0.4 CpG sites per clone (2%) were methylated in wild-type (WT1) spleen cells, whereas averages of 9.1 (48%) and

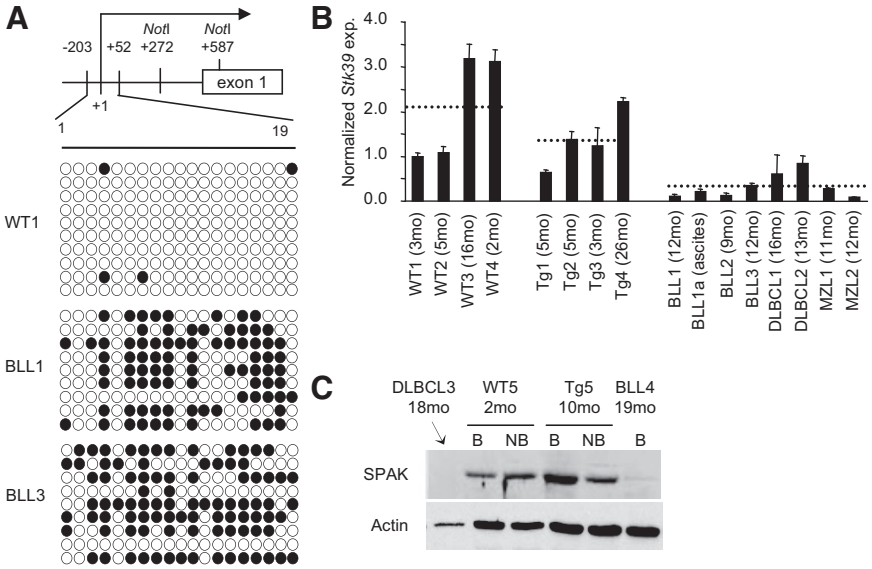

Figure 1. *Stk39* is DNA-hypermethylated, and its expression is repressed in TCL1-tg B-cell lymphomas. **A:** Genomic bisulfite sequencing of part of a *Stk39* promoter region CpG island located between −203 and +52 from the major transcription start site (+1). Each row corresponds to the sequence of an individual clone of wild-type spleen (WT1), BLL1, or BLL3 cells (○, unmethylated CpG sites; ●, methylated sites). **B:** *Stk39* expression in wild-type (1 to 4) spleens, premalignant TCL1-tg (1 to 4) spleens, or TCL1-tg B-cell lymphomas was determined by quantitative PCR. The mean *Stk39* expression for each group is shown by a dashed line. *Stk39* expression was normalized to *36b4* (*Rplp0*) and set to 1.0 for WT1. All samples were analyzed in triplicate, a two-tailed *t*-test was performed to determine statistical significance, and data are plotted as the mean ± SD. **C:** SPAK protein expression was evaluated by Western blot of whole spleen or sorted B- and non-B (NB)-cell fractions, from wild-type spleen (WT5), premalignant TCL1-tg (Tg5) spleen, or TCL1-tg B-cell lymphomas (DLBCL3, BLL4). MZL, marginal zone lymphoma.

8.4 (44%) CpG sites per clone were methylated in BLL1 and BLL3 mouse tumors, respectively. These data validate RLGS results and demonstrate that the *Stk39* promoter is frequently hypermethylated in B-cell lymphomas arising in TCL1-tg mice.

To determine whether promoter methylation correlated with *STK39* expression, the steady-state mRNA level was analyzed by quantitative PCR. When compared with *Stk39* expression in wild-type and premalignant TCL1-tg spleens, tumors with *Stk39* DNA methylation showed an average 5.6-fold reduction in *Stk39* expression (1.73 ± 0.99 vs. 0.31 ± 0.24, $P = 0.003$) (Figure 1B). In contrast, the average *Stk39* expression between wild-type and premalignant TCL1-tg spleens was not statistically different (2.10 ± 1.22 vs. 1.37 ± 0.64, $P = 0.23$). SPAK protein expression was also determined in splenocytes from wild-type, premalignant TCL1-tg, and tumorigenic TCL1-tg mice. Protein lysates from the eight original tumor samples in Figure 1B were unavailable, so newly identified TCL1-tg B-cell tumors confirmed by histology and flow cytometry were used, as described previously.[7] SPAK was expressed in both sorted B and non-B cells from 2 month-old wild-type (WT5) and 10-month-old premalignant TCL1-tg (Tg5) spleens (Figure 1C). In contrast, SPAK was not detected in cells from an 18-month-old TCL1-tg splenic tumor (diffuse large B-cell lymphoma [DLBCL] 3) and was markedly repressed in malignant B and non-B cells from a 19-month-old TCL1-tg tumor (BLL4). Four additional splenic TCL1-tg B-cell lymphomas showed a similar loss of SPAK expression (Supplemental Figure S1, see *http://ajp.amjpathol.org*). Combined, these data indicate that SPAK expression is repressed in TCL1-tg B-cell lymphomas that also show promoter region DNA hypermethylation.

Expression of SPAK Is Repressed in Human B-Cell Lymphomas

To evaluate whether SPAK repression also occurs in human tumors, a panel of 42 paraffin-embedded formalin-fixed human B-lymphoma samples were examined for SPAK expression by immunohistochemistry (IHC). Stained sections of hyperplastic tonsil showed stronger SPAK expression in follicular center cells compared with mantle and interfollicular zone cells (Figure 2A). In addition, B cells from tonsil were sorted into naive, GC, and memory subsets, with a Western blot showing SPAK expression throughout mature, nonmalignant B-cell development (Figure 2B). SPAK expression was determined in Burkitt lymphoma ($n = 4$), DLBCL ($n = 11$), follicular lymphoma ($n = 11$), marginal zone lymphoma ($n = 6$), mantle cell lymphoma ($n = 5$), and small lymphocytic lymphoma ($n = 5$). The range of SPAK expression was wide, as shown by a strongly positive marginal zone lymphoma sample (Figure 2C) and a negative small lymphocytic lymphoma sample (Figure 2D). Samples were scored by two pathologists for the percentage of SPAK-expressing tumor cells on a scale ranging from 0 (negative) to 4+ (75 to 100% positive tumor cells) in increments of 25%. For comparison, tonsil shows between 50 to 100% (3+ to 4+) SPAK-positive cell staining as a reference. All of the lymphoma subtypes, with the exception of Burkitt lymphoma, had at least one SPAK negative (0) sample (Figure 2E). All five small lymphocytic lymphoma samples had <50% SPAK-positive tumor cells. Average SPAK expression was highest for the Burkitt lymphoma samples (3.0 ± 0.8), followed by DLBCL (2.4 ± 1.5), marginal zone lymphoma (2.3 ± 1.6), follicular lymphoma (1.4 ± 1.6), mantle cell lymphoma (1.2 ± 1.3), and small lymphocytic lymphoma (1.2 ± 0.8). The loss of SPAK expression may reflect the progression from SPAK-positive B cells, such as in the tonsil, to SPAK-negative tumor cells over time. Samples that have an intermediate amount of tumor cell staining may reflect an intermediate stage in tumor evolution and a heterogeneous population of normal and lymphoma B cells, but this theory will require further investigation. Overall, these results indicate that 34 of 42 (81%) B lymphoma samples contained at least 25% tumor cells lacking SPAK expression (Figure 2F), suggesting that SPAK repression may

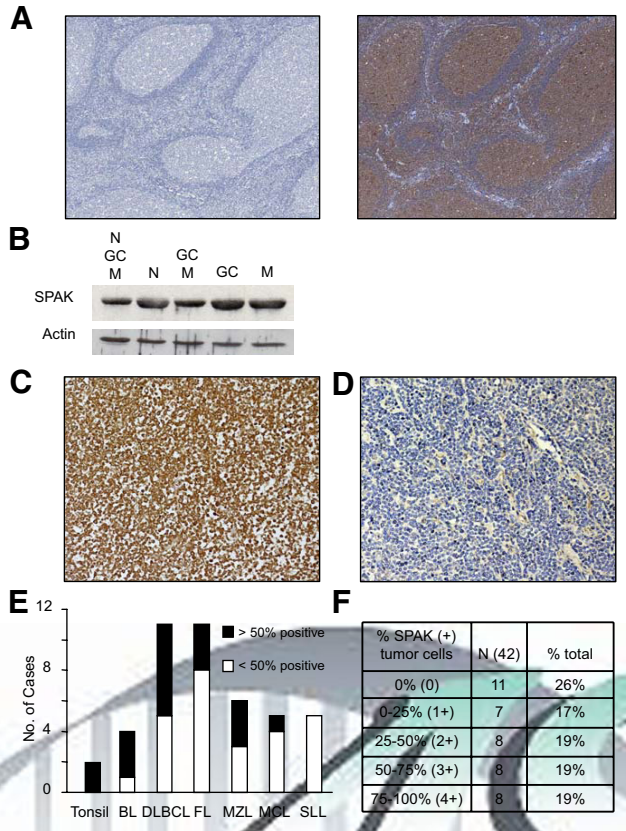

% SPAK (+) tumor cells	N (42)	% total
0% (0)	11	26%
0-25% (1+)	7	17%
25-50% (2+)	8	19%
50-75% (3+)	8	19%
75-100% (4+)	8	19%

Figure 2. SPAK expression is repressed in human B-cell lymphomas. **A:** Immunohistochemistry for SPAK expression in a reactive tonsil GC (original magnification, ×5). **Left panel** is secondary HRP antibody-alone control, and **right panel** is incubated with anti-SPAK antiserum. **B:** Western blot for SPAK expression in naive (N), GC, and memory (M) B cells sorted from tonsil. **C:** SPAK immunohistochemistry in a marginal zone lymphoma expressing SPAK in 75 to 100% of tumor cells (original magnification, ×200). **D:** SPAK immunohistochemistry in a SPAK-negative small lymphocytic lymphoma (original magnification, ×200). **E:** Histogram of 42 human B-cell lymphomas showing cases with >50% (■) or <50% (□) SPAK-positive tumor cells by IHC. **F:** Summary table of immunohistochemical analysis for SPAK expression from **E.**

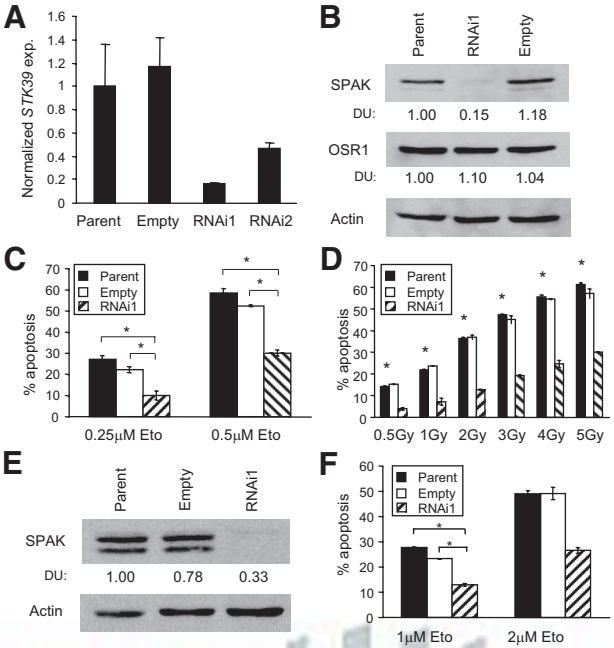

Figure 3. Loss of SPAK protects B cells from apoptosis induced by DNA double-strand breaks. **A:** *STK39* expression in Nalm6 B cells at 2 weeks after infection with empty-vector, RNAi1, or RNAi2 retroviruses was determined by quantitative PCR. *STK39* expression was normalized to *36B4 (Rplp0)* and set to 1.0 for parent Nalm6 cells. Samples were analyzed in triplicate, and data shown are representative of four independent experiments. **B:** SPAK, OSR1, and actin expression was evaluated by Western blot in Nalm6 cells from **A.** Densitometry units (DU) are displayed as intensity of SPAK or OSR1, normalized to actin. Data shown are representative of three independent experiments. **C:** At 24 hours after treatment with 0.25 or 0.5 μmol/L etoposide (Eto), control and RNAi1 Nalm6 cells were evaluated for apoptosis by flow cytometry. Each bar graph represents the percent annexin V^+ cells in the treated sample minus that in an untreated sample control. Samples were analyzed in triplicate, and data shown are representative of eight independent experiments. $^*P < 0.05$. **D:** Control and RNAi1 Nalm6 cells were treated with escalating doses of IR, rested for 18 hours, and evaluated for apoptosis as in **C.** Samples were analyzed in triplicate, and data shown are representative of eight independent experiments.$^*P < 0.05$. **E:** SPAK expression was evaluated by Western blot in BCBL1 cells infected with empty-control or RNAi1 retroviruses after 2 weeks of puromycin selection. Data shown are representative of two independent experiments. **F:** At 24 hours after treatment with two doses of Eto, control and RNAi1 BCBL1 cells were evaluated for apoptosis by flow cytometry. Each bar graph represents the percent annexin V^+ cells in the treated sample minus that in an untreated sample control. Samples were analyzed in triplicate, and data shown are representative of five independent experiments. $^*P < 0.05$.

be a progressive feature of murine and human B-cell lymphomas.

STK39 showed sparse DNA methylation in just 2 of 20 (10%) DLBCL and 0 of 20 follicular lymphoma samples, as determined by methylation-specific PCR and sample-selected genomic bisulfite sequencing (data not shown). This lack of DNA methylation, coupled with progressive SPAK silencing, suggests that there are distinct pathways for human B-cell lymphomas and mouse TCL1-tg B-cell lymphomas in repressing SPAK expression. Consistent with this result, loss of SPAK expression in metastatic prostate and treatment-resistant breast cancers has not been linked to aberrant DNA methylation,[13,14] suggesting another silencing mechanism in humans that requires further investigation.

Loss of SPAK Protects B Cells from Apoptosis Induced by DNA Double-Strand Breaks

To investigate a role for repressed SPAK expression in B-cell lymphoma, nonoverlapping *STK39*-targeted shRNA retroviral constructs were tested, with one knockdown construct generated against a previously published target region of *STK39* (RNAi2)[18] and the other constructed using a newly selected targeted region (RNAi1). Virus was generated and used to infect human Nalm6 B cells. Nalm6 cells were chosen because they expressed SPAK and tolerated retroviral infection to generate stable *STK39* knockdown B cells, whereas unstimulated primary B cells died in culture by 7 days. At 2 weeks after infection *STK39* expression was reduced by 85% ($P = 0.02$) with RNAi1 or 53% ($P = 0.05$) with RNAi2 compared with that in parent cells (Figure 3A). SPAK protein expression with RNAi1 infection was also markedly reduced compared with that in control cells (Figure 3B). Despite 74% sequence identity between SPAK and the only other STE-20 subfamily member, OSR1, RNAi1 showed strong SPAK specificity (Figure 3B). Because of its strong specificity and superior SPAK knockdown compared with a

prior published SPAK knockdown construct (RNAi2),[18] RNAi1 was used for all subsequent studies.

Resting RNAi1 Nalm6 cells seemed unaffected in culture and showed no difference in viability with 3-(4,5-dimethylthiazol-2-yl)-2,5-diphenyltetrazolium assays (data not shown). SPAK has been shown to activate p38 and possibly JNK MAPK pathways in response to osmotic stress,[12,18,20,21] which may cause apoptosis.[22] To determine whether *Stk39* repression impaired B-cell stress responses, Nalm6 cells were challenged with stressors known to activate MAPK signaling. RNAi1 and control Nalm6 cells were treated with escalating doses of sorbitol (hyperosmotic stress), H_2O_2 (oxidative stress), or etoposide (genotoxic stress), with apoptosis determined by annexin V-FITC/propidium iodide staining and flow cytometry. RNAi1 cells were protected from apoptosis at two doses of etoposide compared with parent cells ($P = 0.0005$ and $P = 0.005$) and empty-vector cells ($P = 0.001$ and $P = 0.018$) (Figure 3C). In contrast, RNAi1 cells remained sensitive to sorbitol and H_2O_2 treatments, an unexpected result given the known role of SPAK in regulating apoptosis with hyperosmotic stress (Supplemental Figure S2, A and B, see *http://ajp.amjpathol.org*). A scrambled, nontargeting RNAi construct did not reduce SPAK expression or cause a reduction in apoptosis with sorbitol, H_2O_2, or etoposide treatments (data not shown).

Etoposide is a topoisomerase II inhibitor that blocks DNA DSB repair. To test whether loss of SPAK provides a survival advantage against a second DSB generator, RNAi1 and control cells were treated with escalating doses of IR. Compared with control cells, RNAi1 Nalm6 cells were protected from apoptosis by >50% with 0.5 to 5 Gy IR ($P \leq 0.05$ at every dose) (Figure 3D). RNAi2 Nalm6 cells, with only 53% reduced *STK39* expression (Figure 3A), exhibited no protection from DSBs (Supplemental Figure S3A, see *http://ajp.amjpathol.org*), whereas simultaneously tested RNAi1 cells showed significantly less apoptosis (33.4 ± 0.4%, $P = 0.007$), suggesting that a threshold loss of SPAK expression was reached to protect cells from DSB-induced apoptosis. A third shRNA construct (RNAi3), targeting *STK39* at a region different from those targeted by RNAi1 and RNAi2, was used to produce retrovirus and infect Nalm6 cells. A similar reduction in SPAK expression was seen in RNAi3 Nalm6 cells as was observed in RNAi1 Nalm6 cells (Supplemental Figure S3B, see *http://ajp.amjpathol.org*). RNAi3 Nalm6 cells challenged with etoposide exhibited significantly enhanced protection from apoptosis compared with parent Nalm6 cells, confirming the protective phenotype observed in RNAi1 Nalm6 cells with repressed SPAK expression (Supplemental Figure S3C, see *http://ajp.amjpathol.org*).

To validate these results in an independent human B-cell line, BCBL1 cells were infected with RNAi1 and empty-vector constructs, with the loss of SPAK expression determined by Western blot (Figure 3E). SPAK generated a variable-intensity doublet from BCBL1, Nalm6, and other B-cell lysates, and RNA interference abolished the expression of both bands. At 24 hours of exposure to 1 μmol/L etoposide, 27.8 ± 0.2% of parent versus 13.0 ± 0.4% of RNAi1 infected BCBL1 cells were apoptotic ($P = 0.02$) (Figure 3F). Therefore, SPAK loss inhibited DSB-induced apoptosis in BCBL1 cells, similar to the protection provided to Nalm6 cells.

IR results in the recruitment and activation of ATM to sites of DSBs, followed by ATM phosphorylation of p53 at Ser-15 as part of a cell cycle arrest and DNA repair or apoptosis response.[23] p53 phosphorylation was therefore assessed as a surrogate to determine whether the loss of SPAK was protecting cells from apoptosis by impairing DSB detection or ATM signaling.[24] At 3 hours after IR, p53 Ser-15 phosphorylation was induced to similar levels in control and RNAi1 Nalm6 cells (Supplemental Figure S4, see *http://ajp.amjpathol.org*), strongly suggesting that loss of SPAK interferes with events downstream of ATM activation that induce apoptosis.

To determine whether SPAK loss protected B cells from DNA damage beyond DSBs, RNAi1 cells were challenged with the DNA single-strand breaker, UV-B. At 24 hours of dose-escalating UV-B exposure, no statistical difference was detected between control and RNAi1 cell apoptosis (Supplemental Figure S5, see *http://ajp.amjpathol.org*). The combined data indicate that SPAK specifically protects B cells with DNA DSBs from apoptosis.

SPAK Regulates Caspase 3 Cleavage in Response to Genotoxic Stress

Genotoxic stress can activate MAPK pathways to cause caspase-dependent cell death.[25–27] Because SPAK activates p38 and possibly JNK stress signaling[12,18,20,21] and its repression protects B cells from DNA DSB-induced apoptosis (Figure 3), the dependence of caspase activation on SPAK expression with DNA DSBs was determined. Procaspase 3 was processed to caspase 3 in control cells at 8 hours of etoposide exposure, whereas reduced procaspase 3 processing was detected in RNAi1 Nalm6 cells (Figure 4A). To determine whether SPAK expression changes with etoposide treatment, Nalm6 cells were harvested and Western blotting was performed for SPAK. No change in the level of SPAK expression was detected by densitometric analysis (Supplemental Figure S6, see *http://ajp.amjpathol.org*). Combined, these data suggested that repression of *STK39* expression could protect malignant B cells from DSB-induced apoptosis via reduced executioner caspase 3 activation.

Different cell types vary in their dependence on caspases to execute apoptosis in response to DNA damage.[28] To determine the contribution of caspase activation during apoptosis of Nalm6 cells with DSBs, control and RNAi1 cells were preincubated for 1 hour with the pan-caspase inhibitor Q-VD-OPH (QVD) followed by etoposide treatment and apoptosis determination. Etoposide alone resulted in >50% apoptosis of control cells, with RNAi1 cells showing increased protection from apoptosis (Figure 4B). With QVD treatment only, 4.9 ± 0.3% of parent cells, 4.5 ± 0.3% of empty-vector cells, and 5.0 ± 0.9% of RNAi1 cells were apoptotic. Addition of etoposide to QVD-treated cells did not significantly increase apoptosis, as control and RNAi1 cells displayed

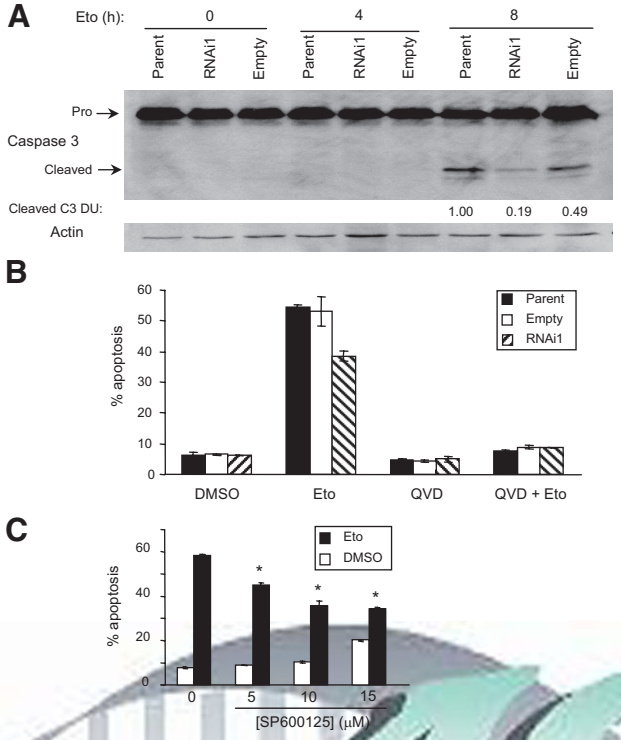

Figure 4. Loss of SPAK results in protection from DNA DSBs via reduced caspase activation. **A:** Cleavage of procaspase 3 (Pro) was assessed by Western blot after exposure to 0.5 μmol/L etoposide (Eto). Densitometry units (DU) are displayed as intensity of cleaved caspase 3 normalized to actin. **B:** Nalm6 cells were or were not preincubated with 20 μmol/L Q-VD-OPH for 1 hour and subjected to 0.5 μmol/L etoposide for 24 hours. Apoptosis was measured by flow cytometry. Percent annexin V^+ is shown. Samples were analyzed in triplicate, and data shown are representative of two independent experiments. **C:** Apoptosis was measured, as in **B,** after a 1-hour preincubation with SP600125 and 24-hour incubation with 0.5 μmol/L etoposide. Samples were analyzed in triplicate, and data shown are representative of four independent experiments. $^*P < 0.05$. DMSO, dimethylsulfoxide.

7.8 ± 0.3, 8.8 ± 0.5, and 8.7 ± 0.1% apoptotic cells, respectively ($P = 0.1$ for all three cell types). Preincubation with QVD resulted in statistically fewer annexin V^+ control and RNAi1 cells compared with the cells that received only etoposide ($P = 0.01$, $P = 0.04$, and $P = 0.03$, respectively). QVD pretreatment also protected control and RNAi1 cells from IR-induced apoptosis (data not shown). Overall, the data indicate that Nalm6 B cells depend on caspase activation to execute apoptosis induced by DSBs. They also suggest that reduced caspase 3 activity in SPAK knockdown cells contributes to reduced apoptosis after DNA DSBs.

Whether SPAK links the regulation of cation chloride cotransporters during osmotic stress signaling to MAPK pathway activation has not been resolved, although p38 activation can be induced by inhibiting the cotransporters NKCC1 and NKCC2 with bumetanide.[29] To assess the contributions of known SPAK target proteins p38, NKCC1, NKCC2, and KCC3 to apoptosis induced by DSBs, pharmacological inhibitors were used. The mitogen-activated protein kinase kinase-1/2 inhibitor U0126 was included as an irrelevant MAPK pathway control because extracellular signal-regulated kinase-1/2 has not been implicated as a SPAK target. The p38 inhibitor (SB203580), JNK inhibitor (SP600125), U0126, and cation cotransporter inhibitors bumetanide and furosemide were used to pretreat Nalm6 cells for 1 hour before 24 hours of etoposide exposure. Inhibition of p38 and extracellular signal-regulated kinase-1/2 failed to protect Nalm6 cells from apoptosis (Supplemental Figure S7, see *http://ajp.amjpathol.org*). In addition, preincubation with dose-escalating bumetanide or furosemide failed to prevent etoposide-induced apoptosis (Supplemental Figure S8, see *http://ajp.amjpathol.org*). Uniquely, pretreatment of Nalm6 cells with SP600125 provided protection from etoposide-induced apoptosis in a dose-dependent manner (Figure 4C). SP600125 alone (15 μmol/L) resulted in 20.2 ± 0.2% apoptotic cells, whereas the addition of 0.5 μmol/L etoposide to pretreated cells yielded 36.9 ± 0.4% apoptotic cells, leaving only 16.7% apoptosis due to etoposide. In contrast, 7.7 ± 0.4% of cells without etoposide were apoptotic, and etoposide treatment yielded 58.3 ± 0.8% apoptotic cells, resulting in 50.6% apoptosis due to etoposide. The amount of apoptosis with etoposide was significantly reduced in a dose-dependent manner from JNK inhibition at 5, 10, and 15 μmol/L SP600125 ($P = 0.04$, $P = 0.05$, and $P = 0.01$, respectively). BCBL1 cells were also similarly protected from etoposide after pretreatment with SP600125 (Supplemental Figure S9, see *http://ajp.amjpathol.org*). Attempts to further support these inhibitor studies by JNK1 and JNK2 knockdown with Dharmacon-predicted/selected RNAi and published sequences were not possible because of <50% knockdown of JNK1 with any tested construct in Nalm6 and BCBL1 B cells (data not shown). Nevertheless, these results in B-cell lymphoma were consistent with recent data from endometrial cancer and Jurkat T cells in which JNK activation regulated apoptosis with etoposide treatment.[30,31] Combined with SPAK activation of JNK,[29] the data suggest that repressed SPAK expression protects B cells from caspase-dependent DSB-induced apoptosis independent of SPAK activity on p38 MAPK and the cation cotransporters NKCC1, NKCC2, and KCC3.

Discussion

This study focused on determining whether loss of SPAK, a member of the STE20 kinase family, has a potential role in B-cell lymphoma progression. The data suggest a potentially broader role in the progression of multiple types of cancer in which SPAK expression is lost. Our prior RLGS survey of genomic loci in B-cell tumors from TCL1-tg mice identified *Stk39* as a candidate target of tumor-specific DNA hypermethylation.[9] Here we show that *Stk39* is DNA-hypermethylated in TCL1-tg but not in human B-cell lymphomas, although SPAK expression is repressed in many TCL1-tg and human B-cell lymphomas. SPAK is known to regulate hyperosmotic cell stress signaling through cation chloride channels and p38 MAPK pathway activation in nonlymphoid cells. In contrast, we show that loss of SPAK protects B cells from DNA DSB-induced apoptosis but has no effect on apoptosis in response to hyperosmotic or oxidative cell stressors, which suggests cell type-specific stress pathway

responses for SPAK. Increased cell survival after DSBs due to loss of SPAK was not linked to cation chloride transporters or p38 MAPK signaling but instead linked SPAK to executioner caspase activation, possibly through JNK. JNK activation has recently been linked to apoptosis after DSBs in endometrial carcinoma and Jurkat T cells,[30,31] also suggesting this mechanistic possibility for SPAK in B-cell lymphomas. Prior microarray studies implicate *STK39* down-regulation by an unknown mechanism in metastatic prostate cancer with tumor relapse[14] and correlate its expression with increased breast cancer responsiveness to genotoxic therapies.[13] Our findings implicate SPAK loss in a third cancer type and, unlike prior studies, identify an unanticipated role for SPAK loss in apoptosis with DNA damage.

B cells require activation-induced cytidine deaminase-initiated DNA breaks and repair within and outside GCs to refine antibody specificity and change isotype.[32] In GCs, the canonical DNA damage response is temporarily dampened to allow rapid B-cell expansion without excessive apoptosis during a robust humoral response. This hiatus is achieved by BCL6-mediated transient repression of *ATR*, *p21*, and possibly *p53* components of the DNA damage response pathway [reviewed in Ref. 32]. Although attenuated, ATM-dependent DNA repair still occurs to correct damage from rapid replication and activation-induced cytidine deaminase-induced *IG* affinity maturation to maintain genome integrity.[33,34] Potentially dangerous B cells must be eliminated by apoptosis to avoid autoimmunity or malignancy.[32] Our data that SPAK is expressed normally in B cells and facilitates DSB-induced apoptosis suggest that SPAK could mediate B-cell apoptosis and elimination of potentially harmful B cells, possibly by JNK-dependent caspase activation. Consistent with this notion, mice deficient in JNK1/2 resist IR-induced apoptosis but retain sensitivity to apoptosis by Fas receptor ligation, further suggesting a selective role for JNK in DSB-induced apoptosis.[35] We propose a model in which the *Stk39* promoter is normally unmethylated and SPAK is expressed. B cells with DNA DSBs are repaired through ATM activation or die by caspase-mediated apoptosis from SPAK-dependent and independent mechanisms, such as Fas. With SPAK repression, probably by distinct mechanisms in mouse and human B-cell lymphomas, B cells can accumulate genetic insults and be increasingly protected from DSB-induced apoptosis, promoting malignancy or malignant progression. In concert with this proposed mechanism, failed repression of *TCL1* as modeled in TCL1-tg mice also reduces Fas-mediated apoptosis and promotes tumor formation. Our model predicts that genotoxic therapies, which require intact death signaling to eradicate tumor cells, would be more effective in tumors expressing SPAK, which has been suggested for breast cancer.[13] Genotoxic therapy also can positively select for cells with repressed genes that are needed for a DNA damage response, which is correlated with *STK39* silencing in aggressive prostate tumor relapse.[14]

SPAK is expressed in T cells and T-cell receptor activation results in SPAK binding to protein kinase Cθ, which activates the JNK downstream target activator protein-1 (AP-1) and leads to cytokine secretion.[18] Our data also suggest the JNK pathway is downstream of SPAK in B cells, although precisely how SPAK regulates JNK signaling in response to DSBs remains to be determined. As a putative MAP4K, SPAK may act through MAP3K and MAP2K upstream of JNK to transmit genotoxic stress signals,[36] and several studies have implicated JNK in apoptosis from IR and genotoxic therapies.[37,38] In addition, etoposide and cisplatin genotoxins cause potent JNK activation, and introduction of dominant-negative MKK4, a MAP2K upstream of JNK, results in cisplatin resistance.[38,39] We speculate that loss of SPAK may affect JNK and caspase activation through MKK4, because MKK4 is a tumor suppressor that is deleted in a subset of metastatic human prostate cancers.[14,40]

Overall, the data presented here suggest that SPAK silencing in B-cell lymphomas promotes cancer progression by crippling genotoxic stress signaling to impair caspase activation. These results probably generalize to breast, prostate, and possibly other cancers beyond B lymphoma and uncover a novel role for SPAK in controlling the DNA damage response, highlighting a protective cell death mechanism that is disabled during the progression of cancer. SPAK expression or repression may also help indicate those patient tumors that should or should not receive genotoxic therapies as the development of personalized medicine pushes ahead.

Acknowledgments

We thank Stephen T. Smale, Randolph Wall, and Joshua Deignan for critical analysis of the manuscript and Christine Bonzon and Herbert Eradat for helpful discussions.

References

1. Kuppers R: Mechanisms of B-cell lymphoma pathogenesis. Nat Rev Cancer 2005, 5:251–262
2. Calin GA, Dumitru CD, Shimizu M, Bichi R, Zupo S, Noch E, Aldler H, Rattan S, Keating M, Rai K, Rassenti L, Kipps T, Negrini M, Bullrich F, Croce CM: Frequent deletions and down-regulation of micro-RNA genes miR15 and miR16 at 13q14 in chronic lymphocytic leukemia, Proc Natl Acad Sci USA: 2002, 99:15524–15529
3. Costello JF, Fruhwald MC, Smiraglia DJ, Rush LJ, Robertson GP, Gao X, Wright FA, Feramisco JD, Peltomaki P, Lang JC, Schuller DE, Yu L, Bloomfield CD, Caligiuri MA, Yates A, Nishikawa R, Su Huang H, Petrelli NJ, Zhang X, O'Dorisio MS, Held WA, Cavenee WK, Plass C: Aberrant CpG-island methylation has non-random and tumour-type-specific patterns. Nat Genet 2000, 24:132–138
4. Shilatifard A: Chromatin modifications by methylation and ubiquitination: implications in the regulation of gene expression. Annu Rev Biochem 2006, 75:243–269
5. French SW, Dawson DW, Miner MD, Doerr JR, Malone CS, Wall R, Teitell MA: DNA methylation profiling: a new tool for evaluating hematologic malignancies. Clin Immunol 2002, 103:217–230
6. Teitell MA: The TCL1 family of oncoproteins: co-activators of transformation. Nat Rev Cancer 2005, 5:640–648
7. Hoyer KK, French SW, Turner DE, Nguyen MT, Renard M, Malone CS, Knoetig S, Qi CF, Su TT, Cheroutre H, Wall R, Rawlings DJ, Morse HC 3rd, Teitell MA: Dysregulated TCL1 promotes multiple classes of mature B cell lymphoma, Proc Natl Acad Sci USA 2002, 99:14392–14397
8. Shen RR, Ferguson DO, Renard M, Hoyer KK, Kim U, Hao X, Alt FW, Roeder RG, Morse HC 3rd, Teitell MA: Dysregulated TCL1 requires

the germinal center and genome instability for mature B-cell transformation. Blood 2006, 108:1991–1998
9. Dawson DW, Hong JS, Shen RR, French SW, Troke JJ, Wu YZ, Chen SS, Gui D, Regelson M, Marahrens Y, Morse HC 3rd, Said J, Plass C, Teitell MA: Global DNA methylation profiling reveals silencing of a secreted form of Epha7 in mouse and human germinal center B-cell lymphomas. Oncogene 2007, 26:4243–4252
10. Delpire E, Gagnon KB: SPAK and OSR1: STE20 kinases involved in the regulation of ion homoeostasis and volume control in mammalian cells. Biochem J: 2008, 409:321–331
11. Piechotta K, Lu J, Delpire E: Cation chloride cotransporters interact with the stress-related kinases Ste20-related proline-alanine-rich kinase (SPAK) and oxidative stress response 1 (OSR1). J Biol Chem 2002, 277:50812–50819
12. Johnston AM, Naselli G, Gonez LJ, Martin RM, Harrison LC, DeAizpurua HJ: SPAK, a STE20/SPS1-related kinase that activates the p38 pathway. Oncogene 2000, 19:4290–4297
13. Cleator S, Tsimelzon A, Ashworth A, Dowsett M, Dexter T, Powles T, Hilsenbeck S, Wong H, Osborne CK, O'Connell P, Chang JC: Gene expression patterns for doxorubicin (Adriamycin) and cyclophosphamide (Cytoxan) (AC) response and resistance. Breast Cancer Res Treat 2006, 95:229–233
14. Hendriksen PJ, Dits NF, Kokame K, Veldhoven A, van Weerden WM, Bangma CH, Trapman J, Jenster G: Evolution of the androgen receptor pathway during progression of prostate cancer. Cancer Res 2006, 66:5012–5020
15. Harris NL, Jaffe ES, Diebold J, Flandrin G, Muller-Hermelink HK, Vardiman J, Lister TA, Bloomfield CD: The World Health Organization classification of neoplastic diseases of the hematopoietic and lymphoid tissues. Report of the Clinical Advisory Committee meeting, Airlie House, Virginia, November, 1997. Ann Oncol 1999, 10:1419–1432
16. Said JW, Hoyer KK, French SW, Rosenfelt L, Garcia-Lloret M, Koh PJ, Cheng TC, Sulur GG, Pinkus GS, Kuehl WM, Rawlings DJ, Wall R, Teitell MA: TCL1 oncogene expression in B cell subsets from lymphoid hyperplasia and distinct classes of B cell lymphoma. Lab Invest 2001, 81:555–564
17. Doerr JR, Malone CS, Fike FM, Gordon MS, Soghomonian SV, Thomas RK, Tao Q, Murray PG, Diehl V, Teitell MA, Wall R: Patterned CpG methylation of silenced B cell gene promoters in classical Hodgkin lymphoma-derived and primary effusion lymphoma cell lines. J Mol Biol 2005, 350:631–640
18. Li Y, Hu J, Vita R, Sun B, Tabata H, Altman A: SPAK kinase is a substrate and target of PKCθ in T-cell receptor-induced AP-1 activation pathway. EMBO J 2004, 23:1112–1122
19. Tao GZ, Rott LS, Lowe AW, Omary MB: Hyposmotic stress induces cell growth arrest via proteasome activation and cyclin/cyclin-dependent kinase degradation. J Biol Chem 2002, 277:19295–19303
20. Piechotta K, Garbarini N, England R, Delpire E: Characterization of the interaction of the stress kinase SPAK with the Na^+-K^+-$2Cl^-$ cotransporter in the nervous system: evidence for a scaffolding role of the kinase. J Biol Chem 2003, 278:52848–52856
21. Polek TC, Talpaz M, Spivak-Kroizman T: The TNF receptor. RELT, binds SPAK and uses it to mediate p38 and JNK activation, Biochem Biophys Res Commun 2006, 343:125–134
22. Xia Z, Dickens M, Raingeaud J, Davis RJ, Greenberg ME: Opposing effects of ERK and JNK-p38 MAP kinases on apoptosis. Science 1995, 270:1326–1331
23. Canman CE, Lim DS, Cimprich KA, Taya Y, Tamai K, Sakaguchi K, Appella E, Kastan MB, Siliciano JD: Activation of the ATM kinase by ionizing radiation and phosphorylation of p53. Science 1998, 281:1677–1679
24. Banin S, Moyal L, Shieh S, Taya Y, Anderson CW, Chessa L, Smorodinsky NI, Prives C, Reiss Y, Shiloh Y, Ziv Y: Enhanced phosphorylation of p53 by ATM in response to DNA damage. Science 1998, 281:1674–1677
25. Chaudhary PM, Eby MT, Jasmin A, Hood L: Activation of the c-Jun N-terminal kinase/stress-activated protein kinase pathway by overexpression of caspase-8 and its homologs. J Biol Chem 1999, 274:19211–19219
26. Davis RJ: Signal transduction by the JNK group of MAP kinases. Cell 2000, 103:239–252
27. Roos WP, Kaina B: DNA damage-induced cell death by apoptosis. Trends Mol Med 2006, 12:440–450
28. Kim R, Emi M, Tanabe K: Caspase-dependent and -independent cell death pathways after DNA damage (review). Oncol Rep 2005, 14:595–599
29. Cheng HF, Wang JL, Zhang MZ, McKanna JA, Harris RC: Role of p38 in the regulation of renal cortical cyclooxygenase-2 expression by extracellular chloride. J Clin Invest 2000, 106:681–688
30. Chen CL, Lin CF, Chang WT, Huang WC, Teng CF, Lin YS: Ceramide induces p38 MAPK and JNK activation through a mechanism involving a thioredoxin-interacting protein-mediated pathway. Blood 2008, 111:4365–4374
31. Reno EM, Haughian JM, Jackson TA, Thorne AM, Bradford AP: c-Jun N-terminal kinase regulates apoptosis in endometrial cancer cells. Apoptosis 2009, 14:809–820
32. Klein U, Dalla-Favera R: Germinal centres: role in B-cell physiology and malignancy. Nat Rev Immunol 2008, 8:22–33
33. Lumsden JM, McCarty T, Petiniot LK, Shen R, Barlow C, Wynn TA, Morse HC 3rd, Gearhart PJ, Wynshaw-Boris A, Max EE, Rodes RJ: Immunoglobulin class switch recombination is impaired in Atm-deficient mice. J Exp Med 2004, 200:1111–1121
34. Reina-San-Martin B, Chen HT, Nussenzweig A, Nussenzweig MC: ATM is required for efficient recombination between immunoglobulin switch regions. J Exp Med 2004, 200:1103–1110
35. Tournier C, Hess P, Yang DD, Xu J, Turner TK, Nimnual A, Bar-Sagi D, Jones SN, Flavell RA, Davis RJ: Requirement of JNK for stress-induced activation of the cytochrome *c*-mediated death pathway. Science 2000, 288:870–874
36. Weston CR, Davis RJ: The JNK signal transduction pathway. Curr Opin Cell Biol 2007, 19:142–149
37. Dent P, Yacoub A, Fisher PB, Hagan MP, Grant S: MAPK pathways in radiation responses. Oncogene 2003, 22:5885–5896
38. Boldt S, Weidle UH, Kolch W: The role of MAPK pathways in the action of chemotherapeutic drugs. Carcinogenesis 2002, 23:1831–1838
39. Sánchez-Pérez I, Perona R: Lack of c-Jun activity increases survival to cisplatin. FEBS Lett 1999, 453:151–158
40. Kim HL, Vander Griend DJ, Yang X, Benson DA, Dubauskas Z, Yoshida BA, Chekmareva MA, Ichikawa Y, Sokoloff MH, Zhan P, Karrison T, Lin A, Stadler WM, Ichikawa T, Rubin MA, Rinker-Schaeffer CW: Mitogen-activated protein kinase kinase 4 metastasis suppressor gene expression is inversely related to histological pattern in advancing human prostatic cancers. Cancer Res 2001, 61:2833–2837